

# Fabrication of *In Situ* Ti/TiC Laminated Composite Material Using Flakes Powder Metallurgy

Mereib D<sup>1,3\*</sup>, Chung UC<sup>3</sup>, Zakhour M<sup>1</sup>, Nakhl M<sup>1</sup>, Doyen NT<sup>2</sup>, Bobet JI<sup>3</sup> and Silvain JF<sup>3</sup>

<sup>1</sup>LCPM/PR2N, Faculté des sciences, Université Libanaise, Lebanon

<sup>2</sup>SPCTS, F-33600 Limoges, France

<sup>3</sup>CNRS, Université de Bordeaux, ICMCB, Pessac, France

## Abstract

Inspiring from the microstructure of natural biological materials and using ball milling (BM) of Ti powder with stearic acid (SA) and the Spark Plasma Sintering (SPS) technique, an *in-situ* TiC/Ti laminated composite material was successfully elaborated. The use of SA during BM induced i) the fabrication of the flakes powder morphology and ii) the formation of TiC amorphous phase. During SPS sintering the flakes powder were assembled into fully dense laminated materials and the TiC phase recrystallized and precipitated in the form of an interlaminar nanometric reinforcement in the dense material. The results show a contribution of 20% and 5% of the TiC in the increase of the hardness and Young's modulus of the material respectively. The control of the BM conditions (BM time and SA amount) allows the control of the TiC content formed *in situ* in the dense Ti/TiC composite material and so of the mechanical properties.

**Keywords:** TiC/Ti composite materials; Laminated materials; Flakes powder metallurgy; Ball milling; Mechanical properties

## Introduction

Titanium matrix composites (TMCs) offer a combination of good mechanical properties and high temperature durability that render them attractive materials for commercial automotive, aerospace and advanced military applications. The incorporation of high strength and high stiffness ceramic reinforcements can improve their mechanical performances [1,2]. Titanium carbide (TiC) has been used for reinforcement of titanium alloy matrices due to its compatibility. Such TMC are commonly called “*ex-situ*” composites. However, large *ex-situ* TiC particles act as stress concentrators in the matrix during tensile loading. This leads to the premature fracture of brittle TiC particles followed by coalescence of micro-cracks initiated from the particulates [3]. Nevertheless, the particulate reinforcement phase can be formed *in-situ* in the Ti matrix. The *in-situ* formation technique offers the advantages of better control of size and level of reinforcement and enhancement of the ceramic-matrix bonding [4-8]. Some studies showed that mixing graphite powder and pure titanium successfully produced TiC nano-particles dispersed in the Ti matrix [4]. Other studies synthesized *in-situ* Ti/TiC composites by consolidation via spark plasma sintering (SPS) of Ti powders with either carbon nanotubes or carbon black [3,5,6]. Other succeeded to disperse nanoscale lamellar TiC particles in a Ti matrix by selective laser melting [9] or combined nano-sphere resol coating Ti powder with conventional powder metallurgy to self-assemble TiC platelets in a Ti matrix [10].

Recently, a novel way to synthesize *in-situ* TiC/Ti composite material, was developed by field assisted hot pressing of a mixture of hexagonal close packed ( $\alpha$ ) (hcp( $\alpha$ )) and face-centered cubic (fcc) powders produced by mechanical milling. During consolidation, the fcc phase decomposes into  $\alpha$ -Ti and dispersed TiC particles [11].

Previous studies show BM of Ti does not only reduce the grain size but also induces phase transformation originates. A metastable fcc solid-state transformation in Ti governed by lattice expansion (negative hydrostatic pressure) as a result of grain refinement during milling, and to contamination with interstitials of C, O and N. It was mentioned that phase transformation was not observed during processing

under an ultrahigh purity environment [12-14]. Large amount of lattice defects and interfaces introduced during milling can increase the free energy of the system and can appropriate an energetically uphill process in the following reactions. In terms of crystallographic relations, the transition from hcp to fcc is possible when a number of stacking faults are introduced on the closed packed planes. This fcc was earlier obtained by BM of Ti and n-Heptane mixture whereby C and H decomposition influences the stabilization of the metastable phase. When many stacking faults are produced in deformed hcp-Ti to realize a fcc structure locally, a metastable compound similar to TiC can be formed by the introduction of C and H atoms accompanying lattice expansion [15].

It was reported that stearic acid (SA) is an 18-carbon chain saturated fatty acid used as process control agent during BM and considered as C source to Ti. Ball milling of titanium mixed stearic acid yields the formation of the metastable fcc phase upon sintering. TiC phase segregating along the grain boundaries due to the reactions between Ti and SA decompose elements was observed [16]. The formation of grain boundary TiC in biomedical titanium alloy due to plastic deformation upon milling that induce the change in crystal structure of Ti was studied [17].

In other side, natural biological materials, such as teeth, bones and mollusk shells are characterized by a layered architecture that exhibits excellent mechanical properties. Inspired from the lamellar architecture of nacre, the efforts were increased for the fabrication of lamellar composite material called biomimetic materials which showed desirable mechanical properties [1-6]. Different techniques are

**\*Corresponding author:** Daa Mereib, CNRS, Université de Bordeaux, ICMCB, France, Tel: +33540002542; E-mail: [daa.mereib@u-bordeaux.fr](mailto:daa.mereib@u-bordeaux.fr)

**Received** July 10, 2018; **Accepted** September 20, 2018; **Published** September 27, 2018

**Citation:** Mereib D, Chung UC, Zakhour M, Nakhl M, Doyen NT, et al. (2018) Fabrication of *In Situ* Ti/TiC Laminated Composite Material Using Flakes Powder Metallurgy. J Powder Metall Min 7: 192. doi:10.4172/2168-9806.1000192

**Copyright:** © 2018 Mereib D, et al. This is an open-access article distributed under the terms of the Creative Commons Attribution License, which permits unrestricted use, distribution, and reproduction in any medium, provided the original author and source are credited.

used for the fabrication of this multilayered architecture materials, a new process called “flakes powder metallurgy” has been used for the fabrication of lamellar MMC materials. The aim of this process is to sinter metallic powder or metallic flakes, prepared by ball milling, with controlled microstructure in order to obtain lamellar architectures [18-20]. Studies have reported that during the early stage of ball milling of ductile metals, and using process control agents such as stearic acid (SA) or ethylen bis-stearamid (EBS) or others, the formation of flakes is observed before the fracture of the powders and can be attributed to plastic deformation of the metallic powder [21].

In the present work, we study the use of ball-milled flakes powder for the fabrication of lamellar *in-situ* TiC/Ti composites material. We discuss the effect of the SA and BM times on (i) the milled powder morphology, (ii) the precipitation of TiC phase after sintering and (iii) the mechanical properties of the sintered materials. In this process, Ti spherical powders were ball-milled for different times with different SA amounts. The powders are then sintered using Spark Plasma Sintering (SPS) technique that allows the fast densification of the Ti. The microstructure and the mechanical properties (elastic and hardness) of the final material are studied.

## Experimental Procedures

### Ti powder elaboration

Titanium flakes powder is obtained by ball milling (BM) using a planetary mill (Fritsch Planetary Mill) using stainless steel balls (diameter 5 and 10 mm) and metallic vials (volume 150 mL). In our work, almost spherical titanium powder (Ti, purity=99.5%, CERAC Inc)d50=(48 μm) is used as the initial material. BM is performed under argon atmosphere at 200 rpm, 20:1 balls to powder ratio. Different amounts of stearic acid (1, 2 and 4 wt.%) were added as process control agent, with 3 mL of isopropanol (IPA). The ball milling was carried out for various times (30, 45, 60 and 75 min).

### Ti powder consolidation

SPS process was chosen as sintering technique DR SINTER LAB Spark plasma sintering system (model SPS 515-S) apparatus was used. A graphite die, covered by carbon felt is used to prepare samples of 10 mm of diameter. The temperature is measured by a k-type thermocouple inserted in the die wall. The sintering process was performed under vacuum using the following conditions: The temperature was raised up to 600°C at 100°C/min and maintained during 10 min with a pressure of 100 MPa applied at room temperature and kept constant during the whole experiment.

### Characterization

The morphology and the microstructure of the materials before and after sintering were studied using a scanning electron microscope (SEM) (TESCAN VEGA) on mechanically polished (surface and cross sections) samples). X-ray spectroscopy (EDX), coupled with SEM, allows the analysis of the chemical composition of the sintered material.

The density of the sintered materials is determined using the Archimedes principle. Samples before and after sintering were characterized by X-ray diffraction (XRD). Powder X-ray diffraction (XRD) patterns were collected on a PA Nalitycal X'pert PRO MPD diffractometer in Bragg-Brentano  $\theta$ - $\theta$  geometry equipped with a secondary monochromator and X'Celerator multi-strip detector. Each measurement was made within an angular range of  $2\theta=8-80^\circ$  and lasted for 34 minutes. Some measurements were made with slow acquisition time (300 s/steps) for more analyze precision. The Cu-K $\alpha$  radiation

was generated at 45 KV and 40 mA ( $\lambda=1.5405\text{\AA}$ ). The hardness of the polished materials was measured using Vickers hardness tester model 452 SVD, at a 50 Kg load and 10 s dwell time. Elastic constants (Young's modulus, shear modulus) were determined at room temperature by ultrasonic pulse, using 10 MHz transducers working in reflection mode on 3 mm thick sample. An elemental micro-analysis CHNS (Thermo Fischer Scientific) was used to determine the C amount in Ti ball-milled powder before and after sintering.

## Results

### SA and BM time effects before sintering

Figure 1 shows the change of titanium powders morphology from irregular to flakes after 30 min of BM. The use of SA and IPA as process control agent during BM prevents the powders cold welding and limits the ball milling effect at micro-forging stage that permits the rather fast elaboration of flakes shape powder.

The Figure 2 shows the XRD patterns of the Ti powders, before and after ball milling. By comparing the XRD patterns obtained for

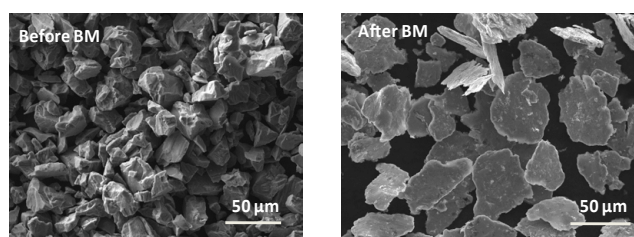


Figure 1: SEM micrographs of Ti powders before BM and after BM 30 min with 2 wt.% of SA.

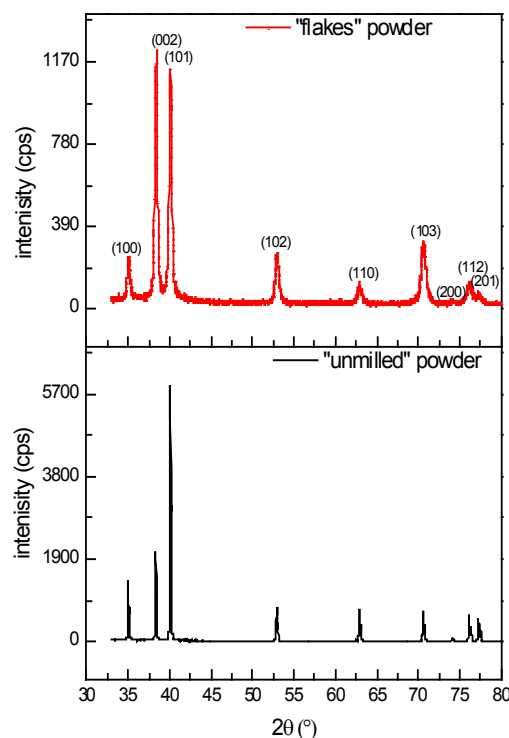


Figure 2: XRD diffraction patterns of Ti “unmilled” and “flakes” powders.

initial powder (“unmilled” powder) and after 30 min of BM (“flakes” powder), we can notice a broadening of the peak and a decrease of their intensities. These two effects can be attributed to the increase of the amounts of crystal defects (dislocations, vacancies), the lattice strains, and to the decrease of the crystallite sizes. Furthermore, after BM process, the relative intensities of the (001) plane become larger than the (hk0) one.

The flakes powder texture represented in the Figure 2 follows the basal plan (002), where the intensity of the (002) plane becomes higher than that of the (101) plane.

Figure 3 shows the effect of SA on the powder morphology after 30 min and 60 min of BM. Without SA, inhomogeneous powder morphology is obtained; some particles are fractured and others still un-fractured with flattened surface. After 60 min the amounts of fractured powder increase. With SA (1, 2 or 4 wt.%) after 30 min of BM, the powder have almost a homogeneous flakes morphology. The flakes aspect ratio (diameter/thickness ratio) doesn't change with the increase of SA amount (Figure 3a). After 60 min of BM (Figure 3b), the morphology of the powder varies according to the amount of SA added. With the increase of SA quantity, the flakes shape is destroyed and fractured powders are formed (Figure 4).

Figure 5 shows the effect of BM times on the morphology of the powder with 2% of SA and 3 ml of IPA. After 30 min, the particles morphology still homogenous; flakes shape powder is obtained. With the increase of ball milling time, the flakes became thinner. After 75 min of BM, the flakes powders are totally fractured in small flakes particle inducing a decrease of the aspect ratio.

### SA amount and BM time effects after sintering

The SPS sintering of Ti ball-milled powder at 600°C, during 10 min under 100MPa of pressure permits to obtain a fully dense material. The cross section view, of the sintered flakes powder, highlights the lamellar architecture obtained. Under a uniaxial pressure, applied during SPS, the Ti flakes orientate and tend to lie flat one on each other leading to an oriented lamellar architecture (Figures 4 and 5b). It's important to noticed that the porosity that appear in the sintered sample is due to the chemical attack that used as metallographic treatment before SEM characterization.

The micrographs MEB BSE, in the Figures 4 and 5b show in some cases two contrasts (light gray and dark gray) in addition to the black contrast related to the grain boundaries. This reveals the formation of a new phase other than Ti after sintering. This phase is essentially

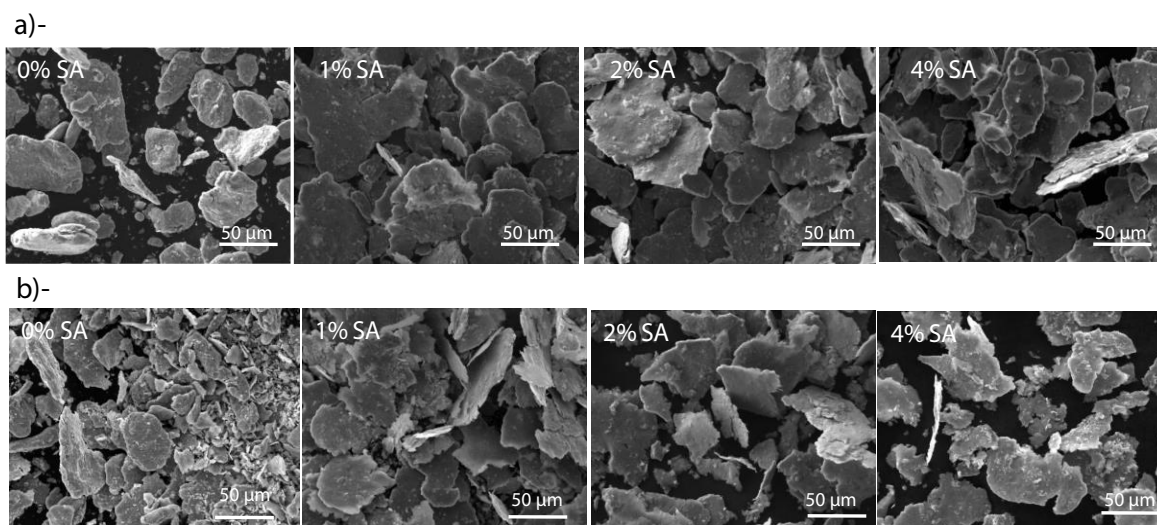


Figure 3: SEM micrographs of Ti ball-milled during a) 30 min and b) 60 min with (0, 1, 2 and 4 wt.% of SA).

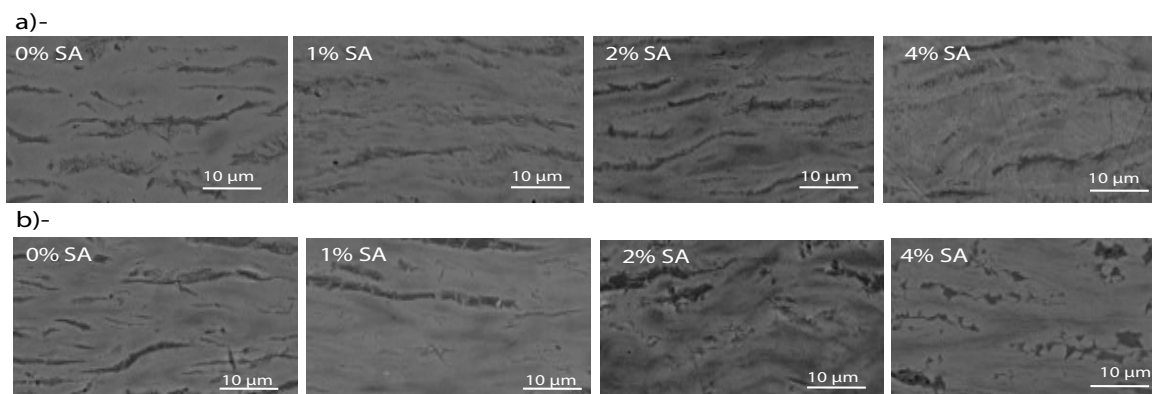


Figure 4: SEM micrographs of Ti ball-milled during a) 30 min and b) 60 min with (0, 1, 2 and 4 wt.% of SA) after sintering at 600°C.

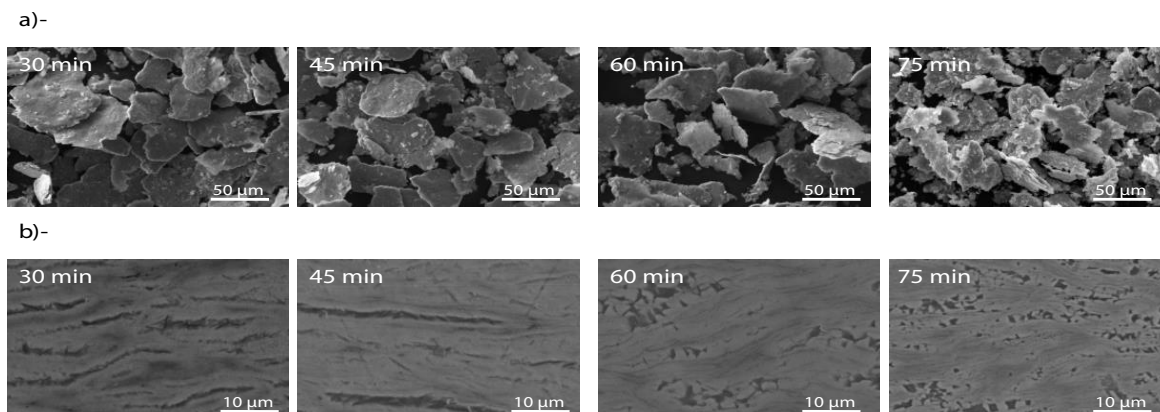


Figure 5: SEM micrographs of Ti ball-milled with 2 wt.% of SA after different BM times (30, 45, 60 and 75 min) before (a) and after (b) sintering at 600°C.

localized around each particle (mainly at the edges of each flake) and acts as inter-lamellar *in-situ* reinforcement (Figure 6). In order to identify the nature of this phase, EDX micrographic analysis with the distribution of Ti and C was performed and shown in Figure 7. It is noted that carbon is located essentially in this new phase as titanium is present everywhere. So it can be concluded that this new phase is composed of Ti and C. On the other hand, the X-rays diffraction pattern, collected by slow acquisition time, indicates the presence of new peaks with low intensities. These peaks can be attributed to the TiC phase. So the new phase represented by the dark gray contrast in the SEM BSE micrographics is the TiC phase.

As shown in the previous paragraph, the presence and the amounts of TiC phase formed after the sintering of ball-milled powder depend on the ball milling conditions (SA amount and BM times). The decomposition of the SA during ball milling is the origin of the C contamination and so of the TiC phase formation.

In order to highlight the ball milling time and SA amount effects, on the elaboration of inter-lamellar TiC reinforcement, the Figures 8 and 9 show the XRD patterns of sintered materials fabricated using flakes powders for different BM conditions. The intensities of XRD peaks characteristic of the hexagonal compact crystal structure of the Ti phase decrease with the increase of BM time at fixed SA amount. This is due to the increase of crystals defaults created by BM. However at fixed BM times (30 or 60 min), with the increase of SA amount, these intensities increase. This is related to the lubricant effect of SA that softened the collisions effect and so the crystals defaults induced by BM.

After 30 min, with 0 and 1% of SA added during BM, no TiC is detected by XRD in the sintered material Figure 8a. However with 2 and 4% of SA small peaks of TiC are observed. In parallel, the SEM BSE of the sintered material confirm the absence of the TiC in the case of the powders ball-milled with 0 and 1% of SA, as with 2 and 4% of SA the dark gray contrast related to the TiC phase is observed (Figure 3b) and it's more pronounced with 2% than 4% of SA.

Likewise, after 60 min of BM, the XRD results of the sintered material (Figure 8b) show the absence of TiC peaks when 0 and 1% of SA are added during BM and their presence with 2 and 4% of SA. In parallel, the SEM BSE micrographic (Figure 4b) show the presence of TiC phase after sintering of the flakes powder prepared with 2 and 4% of SA.

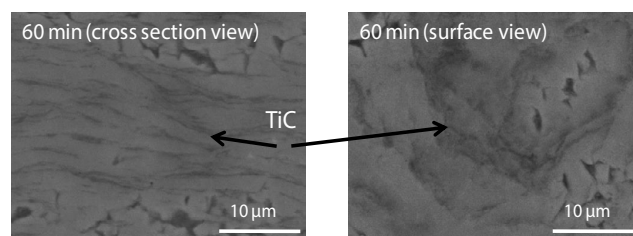


Figure 6: SEM micrographs of Ti ball-milled with 2 wt.% of SA during 60 min after sintering.

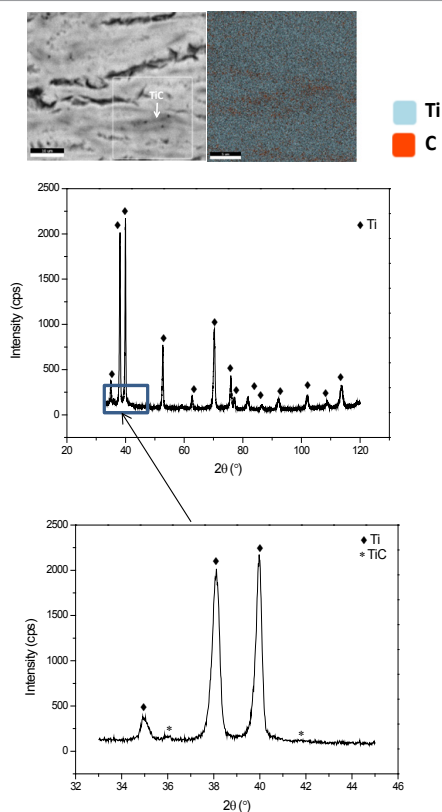
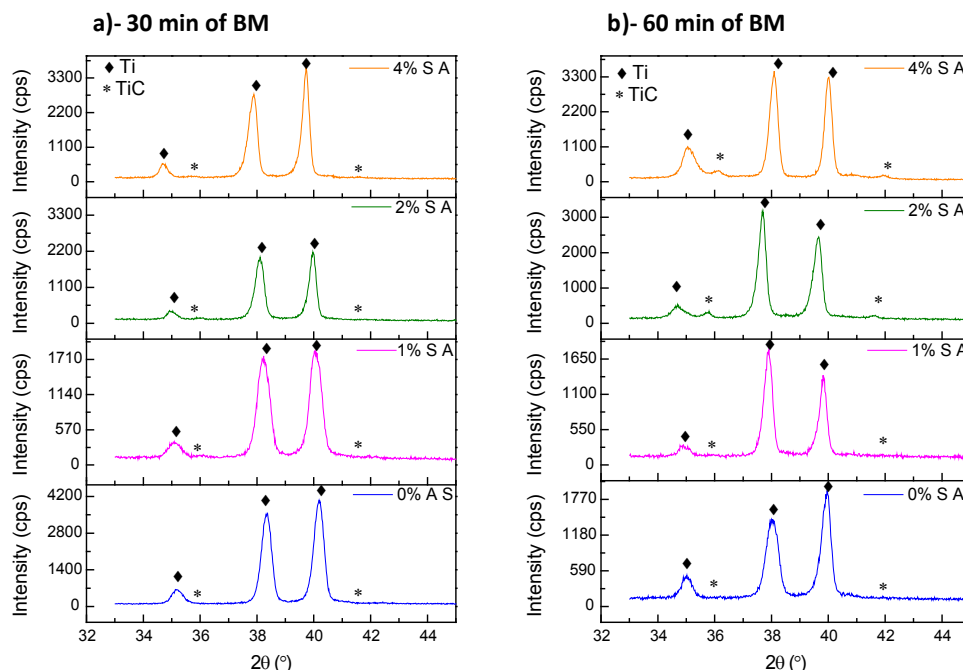


Figure 7: (a) EDX micrographs and (b) XRD diffractions pattern of Ti sintered material, prepared from ball-milled powder with 2 wt.% of SA during 30 min.



**Figure 8:** XRD diffraction patterns of Ti sintered material, prepared from ball-milled powder (a) during 30 min with (0, 1, 2 and 4 wt.%) of SA and (b) during 60 min with (0, 1, 2 and 4 wt.%) of SA.

The Figure 9b presents the XRD pattern of the sintered flakes powder, prepared with 2% of SA for different ball milling times. The intensity of the XRD peaks characteristic of the hexagonal compact crystal structure of the Ti phase, decrease with the increase of BM time. This is due to the increase of crystals defaults created by BM. The TiC peaks appear already after 30 min of BM and even clearly when the BM time increases. This mean, that the increase of BM times, permits additional decomposition of the SA and so the formation of TiC. This result is confirmed by the SEM BSE micrographics, that show the increase of TiC phase contrast with the increase of BM times (Figure 5b).

Figure 10 present the hardness of the sintered material prepared from ball-milled powder obtained from different conditions (different BM time and SA amount). In the case of the material with 60 min ball-milled powder, the hardness varies as a function of SA added amount. This variation is linked with the formation of TiC (Figures 3 and 7). The hardness is maximal with 2wt.% of SA and it slightly decreases with 4wt.% of SA. It increases from 354 Hv to 560 Hv when the BM time increases from 30 to 75 (Figure 10b). This increase is also linked to the increase of the TiC inter-lamellar amount observed in the Figures 5b and 8.

The Young's modulus of the sintered materials prepared from the un-milled Ti powder is consistent with that of pure Ti found in previous studies. However, this modulus increases in the case of materials prepared from ball-milled powder. It even increases from 120GPa to 129GPa when BM times increases from 30 to 60 min. This increase, correlated with the increase in the TiC content, underlines the composite effect of the material. Indeed, the Young's modulus is an intrinsic property independent of the microstructure modifications. The Young's modulus of composite materials obeys the law of mixture. Thus, by measuring the Young's modulus of the Ti/TiC *in-situ* composite material, it is possible to estimate the volume fractions of the reinforcement (V%) TiC precipitated *in-situ* in the Ti matrix knowing

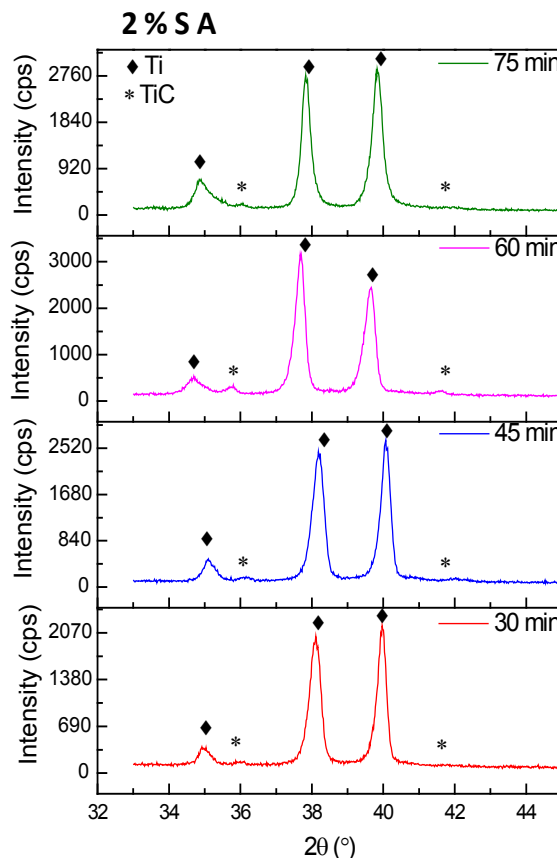


**Figure 9:** XRD diffraction patterns of Ti sintered material, prepared from ball-milled powder with 2 wt.% of SA after different BM times (30, 45, 60 and 75 min).

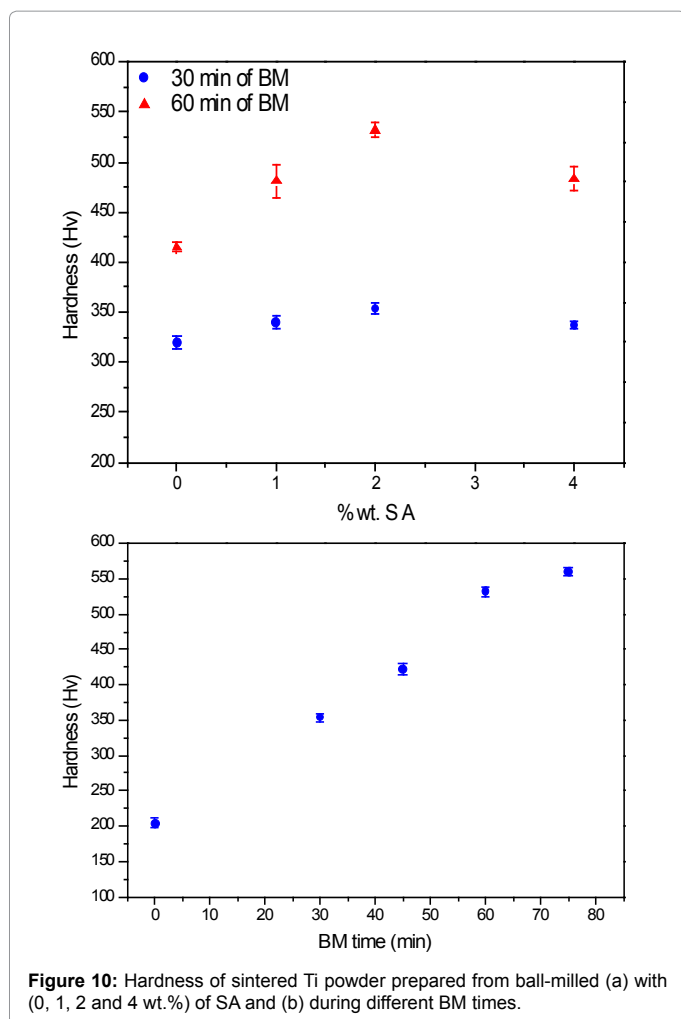


Figure 10: Hardness of sintered Ti powder prepared from ball-milled (a) with (0, 1, 2 and 4 wt.%) of SA and (b) during different BM times.

the Young's modulus of Ti (117 GPa) and TiC=(440 GPa). After 30 min of BM the volume fraction of TiC is close to 1.5% and increases to 4.3% after 60 min (Table 1).

As it has already been mentioned, the carbon responsible of the formation of the TiC after sintering is due to the decomposition of the SA carbon chains during BM. Then, insertion of the C into the Ti takes place during BM. Table 2, resumes the residual C content in the milled powder after heat treatment at 400°C. Such annealing eliminates the entire C on the surface of the material and also the residual SA. Then, the C content measured is the one inserted into the material and which is responsible for the formation of the TiC phase after sintering. The increase of BM time, from 30 to 60 min with 2 and 4% SA, allows additional insertion of C into the material; C content increases from 0.08 to 0.15 wt% and from 0.05 to 0.19 wt% respectively.

## Discussion

### BM time and SA amount effects on flakes morphology

During the BM of ductile material, the powder enters into competition between cold welding and fracture. The mechanical milling process was divided into 5 sequences that started initially by micro-forging flattens ductile powder. Processes control agent (PCA) like IPA and SA are used during the mechanical alloying to avoid the excessive cold welding. This PCA prevents the metal-to-metal contact

BM times (min)	Young's modulus (GPa)	V.% TiC
0	117 ± 2	0
30	122 ± 2	1.5
60	131 ± 2	4.3

Table 1: Young's modulus and TiC volume fraction, of sintered Ti powder prepared from ball-milled powder during different BM times.

Powder ball milling conditions	wt%. of C after 4 h of annealing
30 min of ball milling+2% SA	0.08
60 min of ball milling+2% SA	0.18
30 min of ball milling+4% SA	0.05
60 min of ball milling+4% SA	0.11

Table 2: Wt. % of C in Ti ball-milled powder after annealing under vacuum during 4 h.

surface coating, leading to the limitation of cold welding and increasing fracturing rate. The friction phenomenon decreases considerably when a large amount of PCA is used [1,2]. This explains the fracture of the Ti powder and the inhomogeneous morphology when IPA is added during BM without SA (0% SA). However, when SA is added (1, 2 and 4%) in addition to IPA, the shocks are softened than BM can be seen as micro-rolling of Ti particles without fracture, which allows the formation of flakes morphology observed in Figures 2a and 3a. However, as the BM time increases the flakes become thinner and the fracture can started, and the formation of broken flakes can occur (Figure 5a).

### BM time and SA amount effects on TiC formation

SA is a long carbon chain ( $\text{CH}_3(\text{CH}_2)_{16}\text{COOH}$ ), that decompose into short chains of molecules or radicals, which have a lower boiling point, under thermo-mechanical conditions created by BM. Under these several conditions, the local temperature can be much higher than their boiling temperature, so the SA decomposes and reacts with the Ti milled powder to form carbides (TiC) as showed in Figure 4.

During the BM of Ti the formation of crystalline and stacking defects, the increase of the number of interfaces, the presence of impurities such as C and the refinement of the microstructure (decrease in the size of the crystallites), can lead to an increase in the free energy of the system. This lead to a phase transition from the solid-centered hexagonal crystalline phase (hcp) to a cubic centered face (fcc) metastable phase [11,12]. This transition is governed by the expansion of the crystalline lattice of the compact planes where the C is preferentially localized. The presence of C would stabilize this phase fcc, with a crystallographic correspondence (or equivalence) between the (002) plane of the hcp phase ( $d=0.2342$  nm) and the (111) plane of the fcc phase ( $d=0.2499$  nm). Also the texturing of the "flakes" powder according to the basal plane and its great surface energy would also promote this phase transition [22-24]. To corroborate this hypothesis, we rely on the fact that the solubility limit of C in this phase fcc is lower than in the hcp phase. The formation of TiC particles reflects that the amount of C in solid solution in fcc phase exceed the solubility limit to the hcp phase [11]. This will favor the precipitation of carbon in the form of TiC having a fcc structure [15,16]. This TiC phase is not detected by XRD analysis of the "flakes" powder after BM, which indicates that this phase is amorphous. Heating during SPS sintering, allows the crystallization of this phase (and thus its detection is possible by DRX of the sintered material).

In the case of 1 wt% SA, no TiC XRD peak phase are revealed in the Figure 8a and 8b. Where, the quantity of C isn't enough for the precipitation of TiC phase, but it's still located as solid solution in Ti hexagonal compact crystal structure. However the increase of SA

amount until 2% permits the precipitation of TiC phase as showed from the XRD results in Figure 8a and 8b. The inter-lamellar locations of the carbide phase is due to the Ti flakes surface-Carbon reaction, since that the SA cover the flakes surface. It was reported that maximum carbon solubility is lower than 0.08 wt.% in unalloyed Ti [25]. The Table 2 showed that with 2% SA, the incorporated C amount in Ti milled powder is close (30 min) and higher (60 min) than 0.08 wt.%, hence the precipitation of the carbide.

At 4 wt%SA during 30 min BM, the PCA ensures good lubrication and hence less heat evolution due to the ball collisions. This decrease of local temperatures result in a slower decomposition rate of the SA and so a lower C incorporation, as show in the Table 2. Consequently, no TiC phase is observed (Figures 4a and 8a). The increase of BM time until 60 min, with 4 wt% SA permits the decomposition of higher amount of SA and so the precipitation of TiC phase as showed the Figures 4a and 8b. However the, elaborated TiC phase still lower than that with 2% SA added during 60 BM as showed the intensity of TiC XRD peaks in the Figure 8b and Table 2.

The increase of BM time permits an additional decomposition of SA, and higher crystal defaults (vacancies and dislocations). That induces more C incorporation in the Ti milled powder, and permit a large precipitation of TiC phase in Ti matrix as showed the Figures 5b and 9. The intensity of TiC XRD peaks increases with the increase of BM time, showing the precipitation of high amount of carbide (Figure 9).

### Mechanical properties of sintered ball-milled Ti powder

It was reported in a previous study that the hardness of the sintered Ti material prepared from milled powder is higher than those prepared from un-milled powder. This is related to the work hardening, crystallite size refinement, solid solution strengthening induced by BM [26]. In our study these effects, explain the increase of the hardness of the Ti sintered material made from powder milled without SA and with 1 wt.% SA (Figure 10a), where no TiC precipitation is detected compared to this made from un-milled powder (0 min).

Additional to these effects, the increase of the hardness is linked to the precipitation of inter-lamellar TiC phase in Ti matrix. With the increase of BM time, the kinetic rate of SA decomposition increase and so the incorporation C in the Ti lattice becomes higher. That permits the increase of TiC precipitation in the milled powders, which appear as *in-situ* reinforcements after sintering (Figure 10b). Also, with 2wt% of SA (30 min and 60 min) the TiC precipitation in ball-milled powder is higher than this with 4 wt% as shown from the XRD results of the sintered material, and the C content measured of annealed powder. That fit with hardness variation of the sintered material prepared with 2 and 4 wt% added during BM, where the hardness is higher in the case of 2 wt%.

The TiC reinforcement effect in Ti matrix appears also in the elastic properties of the sintered material. The Young's modulus increase until 131 GPa, for the material made from milled powder during 60 min with 2 wt.% compared to 117 GPa for these prepared from un-milled powder parallel to the increase of TiC inter-lamellar precipitation. That proves the TiC reinforcement effect on the improvement of the titanium matrix stiffness.

### Conclusion

The BM of Ti powder with IPA and SA, allows the fabrication of "flakes" powder with a 2 D morphology, having a texture following the basal plane (002). The SPS sintering of Ti "flakes" powder, at 600°C

under 100 MPa for 10 min, allow the fabrication of a totally dense lamellar material.

As a result of the powder-ball collisions and the increase of the local temperature, the SA breaks up into small carbon chains with a boiling point lower than that of the SA. Part of this carbon, which is located on the surface of the "flakes" powder, evaporates during heating (densification or annealing). The rest of the carbon is inserted as amorphous TiC on the platelet surface. The formation of this TiC phase during BM is induced by: 1) The increase of the local temperature during the BM, 2) The phase transition that the Ti of the hcp phase undergoes in a metastable phase fcc in which the solubility of C is even lower. This TiC phase recrystallizes during sintering and precipitates in the form of an interlamellar nanometric reinforcement in the dense material. The presence of TiC contributes on 20% and 5% to the increase of hardness and Young's modulus of the material respectively. This increase highlights the composite effect of the Ti/TiC *in-situ* material.

The control of the BM conditions (BM time and SA amount) allows the control of the TiC content formed *in-situ* in the dense Ti/TiC composite material. The increase in BM time results in an increase in the TiC content and thus in the hardness and rigidity of the material. The measurement of Young's modulus and the use of the law of the mixtures permit to estimate the rate of TiC formed. Thus, with 2 wt% SA, the increase in BM time from 30 to 60 min induces an increase in TiC from 1.5 to 4.3 V% respectively. Increasing the SA amount by 1 to 2 wt% results in an increase in the TiC amount. On the other hand beyond 2 wt%, the fragmentation of the SA and the phase transition are disadvantaged because of the attenuation of the collision energy and the decrease of the local temperature. Thus a decrease in the TiC level was demonstrated with 4 wt% SA.

### Conflict of Interest Statement

The authors declare that they have no conflict of interest.

### References

1. Tjong SC, Mai YW (2008) Processing-structure-property aspects of particulate- and whisker-reinforced titanium matrix composites. *Compos Sci Technol* 68: 583-601.
2. Brewer WD, Bird RK, Wallace TA (1998) Titanium alloys and processing for high speed aircraft. *Mater Sci Eng A*: 243: 299-304.
3. Kondoh K, Threrujirapapong T, Imai H, Umeda J, Fugetsu B (2009) Characteristics of powder metallurgy pure titanium matrix composite reinforced with multi-wall carbon nanotubes. *Compos Sci Technol* 69: 1077-1081.
4. Liu H, Yao B, Wang L, Wang A, Ding B, et al. (1996) In situ formation of nanometer size TiC reinforcements in Ti matrix composites. *Mater Lett* 27: 183-186.
5. Kondoh K, Threrujirapapong T, Imai H, Umeda J, Fugetsu B (2008) CNTs/TiC Reinforced Titanium Matrix Nano composites via Powder Metallurgy and Its Microstructural and Mechanical Properties. *J Nanomater* 76: 1-4.
6. Kondoh K, Threrujirapapong T, Umeda J, Fugetsu B (2012) High-temperature properties of extruded titanium composites fabricated from carbon nanotubes coated titanium powder by spark plasma sintering and hot extrusion. *Compos Sci Technol* 72: 1291-1297.
7. Morsi K, Patel VV (2007) Processing and properties of titanium-titanium boride (TiBw) matrix composites a review. *J Mater Sci* 42: 2037-2047.
8. Tjong SC, Ma ZY (2000) Microstructural and mechanical characteristics of in situ metal matrix composites. *Mater Sci Eng R Rep* 29: 49-113.
9. Gu D W, Meiners YC, Hagedorn K, Wissenbach, Poprawe R (2010) Bulk-form TiC x /Ti nanocomposites with controlled nanostructure prepared by a new method: selective laser melting. *J Phys Appl Phys* 43: 295-402.
10. Luo SD, Li Q, Tian J, Wangd C, Yana M, et al. (2013) Self-assembled, aligned

- TiC Nano platelet-reinforced titanium composites with outstanding compressive properties. *Scr Mater* 69: 29-32.
11. Manna I, Chattopadhyay PP, Nandi P, Banhart F, Fecht HJ (2003) Formation of face-centered-cubic titanium by mechanical attrition *J Appl Phys* 93: 1520-1524.
  12. Seelam UMR, Barkhordarian G, Suryanarayana C (2009) Is there a hexagonal-close-packed (hcp)  $\rightarrow$ face-centered-cubic (fcc) allotropic transformation in mechanically milled Group IVB elements? *J Mater Res* 24: 3454-3461.
  13. Phasha MJ, Bolokang AS, Ngoepe PE (2010) Solid-state transformation in Nano crystalline Ti induced by ball milling. *Mater Lett* 64: 1215-1218.
  14. Srinivasarao B, Torralba JM, Jabbari Taleghani MA, Pérez-Prado MT (2014) Very strong pure titanium by field assisted hot pressing of dual phase powders. *Mater Lett* 123: 75-78.
  15. Suzuki TS, Nagumo M (1995) Metastable intermediate phase formation at reaction milling of titanium and n-heptane. *Scr Metall Mater* 32: 1215-1220.
  16. Bolokang AS, Motaung DE, Arendse CJ, Muller TFG (2015) Formation of the metastable FCC phase by ball milling and annealing of titanium–stearic acid powder. *Adv Powder Technol* 26: 632-639.
  17. Yan M, Qian M, Kong, MS Dargusch (2014) Impacts of trace carbon on the microstructure of as-sintered biomedical Ti–15Mo alloy and reassessment of the maximum carbon limit. *Acta Biomater* 10: 1014-1023.
  18. Fan G, Xu R, Tan ZD, Zhang, Li Z (2014) Development of Flake Powder Metallurgy in Fabricating Metal Matrix Composites: A Review. *Acta Metall Sin Engl Lett* 27: 806-815.
  19. Jiang L, Li Z, Fan G, Cao L, Zhang D (2012) The use of flake powder metallurgy to produce carbon nanotube (CNT)/aluminum composites with a homogenous CNT distribution. *Carbon* 50:1993-1998.
  20. He W, Li C, Luan B, Qiu R, Ke W, et al. (2015) Deformation behaviors and processing maps of CNTs/Al alloy composite fabricated by flake powder metallurgy. *Trans Nonferrous Met Soc China* 25: 3578-3584.
  21. Benjamin JS, Volin TE (1974) The mechanism of mechanical alloying. *Metall Trans* 5: 1929-1934.
  22. Nouri A, Hodgson PD, Wen CE (2010) Effect of process control agent on the porous structure and mechanical properties of a biomedical Ti–Sn–Nb alloy produced by powder metallurgy. *Acta Biomater* 6: 1630-1639.
  23. Phasha MJ, Bolokang AS, Ngoepe PE (2010) Solid-state transformation in nanocrystalline Ti induced by ball milling. *Mater Lett* 64: 1215-1218.
  24. Phasha M, Maweja K, Babst C (2010) Mechanical alloying by ball milling of Ti and Mg elemental powders: Operation condition considerations. *J Alloys Compd* 492: 201-207.
  25. ASTM F67-13 (2017).
  26. Nouri A, Hodgson PD, Wen C (2011) Effect of ball-milling time on the structural characteristics of biomedical porous Ti–Sn–Nb alloy. *Mater Sci Eng C* 31: 921-928.